49th IEEE Conference on Decision and Control
December 15-17, 2010
Hilton Atlanta Hotel, Atlanta, GA, USA

A Geometric Transversals Approach to Analyzing Track Coverage of Omnidirectional Sensor Networks for Maneuvering Targets

Brian Bernard and Silvia Ferrari

Abstract— **The quality of service of a sensor network performing cooperative track detection can be expressed as the probability of obtaining multiple elementary detections over time, along a target track, also known as track coverage. Recently, distributed search theory and geometric transversals have been used to obtain the probability of track detection for targets traveling with constant speed and heading in a region-of-interest in closed form, as a function of the sensors' ranges and positions, and of the track parameters. In this paper, an extended approach based on convex theory and computational geometry is presented to obtain a track coverage function for maneuvering targets in the plane. In many tracking applications, a maneuvering target is modeled as a Markov motion process with known transition probability functions that are estimated via Kalman filtering from prior sensor measurements. The approach presented in this paper uses line transversals and planar geometry to derive the track coverage of a heterogeneous sensor network as a function of the Markov transition probability functions. The theoretical results are validated through numerical Monte Carlo simulations involving multiple omnidirectional mobile sensors that are deployed to cooperatively detect, track, and eventually pursue one or more maneuvering targets.**

I. Introduction

A well-known objective function used to represent the quality of service of wireless sensor networks is *area coverage*, which represents the probability that a point in a compact subset of a two-dimensional space, referred to as region-of-interest, is within the range of at least one sensor in the sensor network [1]. Depending on the underlying physics, the area coverage of one sensor is the area of a circle or sector centered at the sensor location. Then, the network coverage can be analyzed and optimized by considering the union of all the areas covered by its sensors [2]. Another well-known formulation of coverage is the *art-gallery problem*, where a point or sensor sees the target if the line segment between them does not intersect any obstacles [3]–[5]. This problem, also known as line-of-sight visibility, is concerned with placing the sensors such that the targets in a given area of interest that includes obstacles are in the line-of-sight of at least one of the sensors. In order to address coverage as it pertains to target tracking by means of multiple sensors, so-called *track coverage* functions representing the probability of obtaining multiple elementary detections over time, along a target track, have been proposed in [6]–[8].

The motivation for deriving coverage function expressing the quality of service of wireless sensor networks in closed form is that they can be utilized to optimally deploy mobile sensors, via control theory and algorithms [2], [8]–[10]. Modern embedded systems and technologies are producing networked surveillance systems in which both the sensors and their platforms are characterized by a high degree of functionality and reconfigurability. For example, ground and aerial robots with on-board sensors may be employed for monitoring urban environments, or unauthorized intruders by operating cooperatively, in cluttered dynamic environments with little prior information or human intervention. Existing track coverage functions have been successfully utilized in deployment, control, and coordination algorithms to significantly increase the effectiveness of the sensor network by controlling and, in some cases, optimizing quality of service with respect to the sensors' positions [1], [8]–[16]. However, the main limitation of existing track coverage functions is that they assume that the targets travel with constant heading and speed [8], or that the sensors are uniformly distributed and have constant range [6], [7].

The track coverage function derived in this paper relaxes these assumptions by extending the geometric transversals approach in [8] to a three-dimensional Euclidian space representing the sensor-target spatio-temporal coordinates, in which the Markov parameters of maneuvering targets can be represented by three-dimensional cones finitely generated by the sensors' fields-of-view. There is considerable precedence in the sensor tracking and estimation literature for modeling target tracks by piece-wise Markov motion models in order to estimate the target state from multiple, distributed sensor measurements [17]. Although the transition probability density functions of these Markov models are routinely outputted by tracking and estimation algorithms [17], little work has been done to use them as a feedback to sensor coordination and control algorithms. The new track coverage function presented in this paper provides a closed-form representation of the probability of track detection as a function of these transition probabilities, and accounts for the spatio-temporal trajectories of the sensors and the targets, for any sensor dynamics, and any form of the target probability density functions.

The remainder of the paper is organized as follows. The problem formulation and assumptions are stated in Section II. The geometric approach to analyzing track coverage of maneuvering targets is presented in Section III. The numerical simulations used to validate the theoretical results are provided in Section IV.

B. Bernard and S. Ferrari are with the Laboratory for Intelligent Systems and Controls (LISC), Department of Mechanical Engineering, Duke University, Durham, NC 27708-0005, {brian.bernard, sferrari}@duke.edu

II. Problem Formulation and Mathematical Models

This paper considers a network of n cooperative heterogeneous sensors installed on mobile platforms that are deployed in a region-of-interest (ROI) for the purpose of detecting an unknown number of moving targets during a time interval $[t_0,\ t_f]$. The end time t_f is fixed, and is defined as the maximum time on station achievable by the sensor network. The ROI $\mathcal{A} \subset \mathbb{R}^2$, is assumed to be unbounded. It is assumed that sufficient distance and depth separation will be achieved so that risk of collision between sensors and targets is negligible. This allows the sensors and targets to be modeled as point masses rather than geometric objects. Each sensor is equipped with an isotropic or omnidirectional sensor with a field-of-view (FOV) represented by a disk $\mathcal{C}_i(t) = \mathcal{C}[s_i(t), r_i] \in \mathcal{A}$ that has a constant radius r_i, and is centered at s_i at time t. The set of all sensors is $S = \{\mathcal{C}_1, \ldots, \mathcal{C}_n\}$, and I_S is the index set of S.

In this paper, it is assumed that the i^{th} sensor's position, s_i, is a deterministic and known function of time. The dynamic equation of the sensor, $\dot{s}_i = f(s_i, u_i, t)$, is assumed known and, thus, can be integrated to provide the sensor trajectory, $s_i(t) = [s_{x_i}(t)\ s_{y_i}(t)]^T$ for all $t \in [t_0,\ t_f]$, and $i = 1, ..., n$. In this paper, the dynamics of sensor i are modeled by the nonholonomic unicycle model,

$$\begin{aligned} \dot{s}_{x_i} &= \nu_i \cos\varphi_i, \\ \dot{s}_{y_i} &= \nu_i \sin\varphi_i, \\ \dot{\varphi}_i &= \omega_i, \end{aligned} \tag{1}$$

where, φ_i is the sensor's heading. The control input to sensor i is given by its translational and rotational velocities, $u_i = [\nu_i \quad \omega_i]^T$, and is assumed given.

Targets are assumed to obey the same continuous-time Markov process defined as follows [18]:

Definition 1: A continuous-time random process is a family of random variables x_t where $t \in [0,\ t_f]$.

Definition 2: A random process is said to be continuous with respect to time and Markovian if for $0 \leq t_0 < \cdots < t_{k-1} < t_k < t$ we have $\Pr\{x_t \in B | x_k = X_k, x_{k-1} = X_{k-1}, \cdots, x_0 = X_0\} = \Pr\{x_t \in B | x_k = X_k\}$ where Pr denotes the probability function, and $X_0, \ldots, X_k \in \mathcal{X}$ are realizations of the state space $\mathcal{X}$.

Let the random variables θ and v represent the target's heading and velocity, respectively. Assuming the target's heading and velocity are constant during every interval $\Delta t_j = (t_{j+1} - t_j)$, $j = 1, 2, \ldots$, where Δt_j is not necessarily constant, the target motion can be modeled as a continuous-time Markov process. A three-dimensional real-valued vector function maps the family of random variables $\{\theta_j(t), v_j(t)\}$ into the random vector $p_j(t)$ at every time $t \in [t_0,\ t_f]$, such that the target motion process is,

$$\begin{aligned} \dot{x}_j(t) &= v_j(t)\cos\theta_j(t) \\ \dot{y}_j(t) &= v_j(t)\sin\theta_j(t),\ \ j = 1, 2, \ldots \end{aligned} \tag{2}$$

and, therefore, the motion of target j is a Markov process. The third component of the vector function is the identity

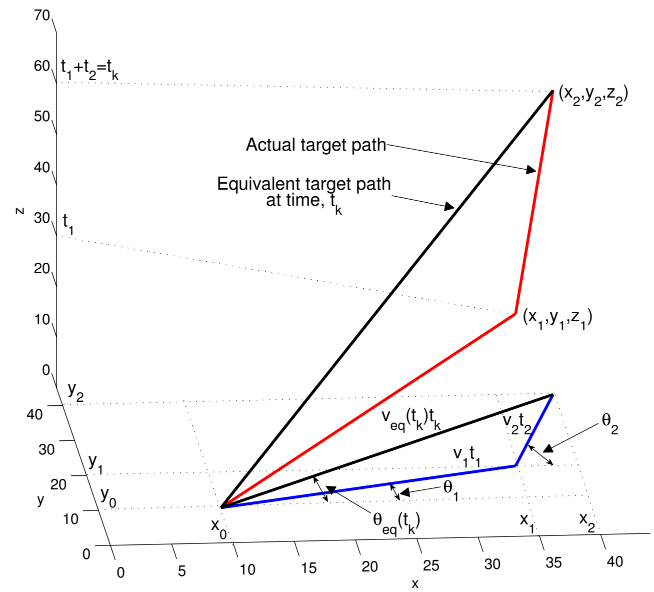

Fig. 1. Target path as a function of time (red), in the Cartesian plane (blue), with the equivalent course/distance vectors (black).

function. Thus, θ_j and v_j are piece-wise constant, as illustrated in Fig. 1, while x_j and y_j have discontinuities at the time instants t_j, $j = 1, \ldots, \rho$, when target j changes its heading and velocity.

Let $\{p_{0_j}\}_{j=1,\ldots,\rho}$ denote the set of target positions at which these discontinuities occur. Then, by integrating the linear differential equation (2) over every interval Δt_j with initial condition p_{0_j}, the position of the j^{th} target at any time t can be obtained as a function of the sequence of random variables $\{p_{0_j}, v_j, \theta_j\}_{j=1,\ldots,\rho} \equiv \{\mathcal{M}_j\}_{j=1,\ldots,\rho}$ also known as Markov motion parameters,

$$p_j(t) = p_{0_j} + v_j(t - t_j)[\cos\theta_j\ \ \sin\theta_j]^T,\ \ t_j \leq t < t_{j+1} \tag{3}$$

where, the Markov motion parameter values $\mathcal{M}_j$ only depend on the values of the previous time step $\mathcal{M}_{j-1}$, and remain constant during the time interval Δt_j. It follows that the target motion is properly represented by the joint probability density function on $\mathcal{M}_j$, i.e., $\Pr(p_{0_j}, \theta_j, v_j, t_j)$ which is known from tracking and estimation algorithms assimilating prior detections in the target motion model. The range of parameters is assumed known from the target and problem characteristics, and is defined by the minimum and maximum target headings, θ_{min} and θ_{max}, the minimum and maximum target speeds, v_{min} and v_{max}, and the final time t_f, where $t_f \geq \sum t_j$. Furthermore, it is assumed that the i^{th} sensor has a non-zero probability to *detect* the j^{th} target at time t if and only if its FOV intersects the target's center of mass, i.e., $\mathcal{C}_i(t) \cap p_j(t) \neq \varnothing$.

The track coverage of the sensor network is derived in the next section, and demonstrated through numerical simulations in Section IV.

III. Methodology

The geometric transversals approach first proposed in [8] analyzes the track coverage of a sensor network facing targets that can move only along straight paths. Each sensor's detection range specifies a detection disk, from which coverage cones can be generated for each potential starting location of the target. The following method extends this technique to maneuvering targets by utilizing 3D coverage cones in a spatio-temporal subset of the Euclidian space $\Omega \equiv \mathcal{A} \times [t_0,\ t_f] \subset \mathbb{R}^3$. Since during every time interval Δt_j the target motion in Ω is linear, it can be represented by a course/speed/time (CST) vector that represents the target location at t_{j+1}, with respect to its position at t_j which also is a Markov parameters and a point of discontinuity in the target path. The CST vector can be conveniently represented in cylindrical coordinates $(\theta_{eq}, v_{eq}, z_{eq})$, where $r_{eq} = v_{eq} t_{eq}$, as follows:

$$\begin{aligned} \theta_{eq} &= \tan^{-1}\left[\frac{\sum_{j=1}^{m} v_j t_j \sin\theta_j}{\sum_{j=1}^{m} v_j t_j \cos\theta_j}\right] \qquad (4) \\ v_{eq} &= \left[\frac{\sqrt{(\sum_{j=1}^{m} v_j t_j \cos\theta_j)^2 + (\sum_{j=1}^{m} v_j t_j \sin\theta_j)^2}}{\sum_{j=1}^{m} t_j}\right] \\ t_{eq} &= \sum_{j=1}^{m} t_j \end{aligned}$$

The probability of obtaining multiple detections by a cooperative, omnidirectional sensor network, referred to as track coverage, was recently obtained for targets that are assumed to travel along straight paths in [8]. In this paper, a novel probability function representing the track coverage for unauthorized targets with a Markov motion process (Section II) is derived using convex theory and geometric transversals (see [19] for a comprehensive review):

Definition 3: A family of k convex sets in $\mathbb{R}^c$ is said to have a d-transversal *if it is intersected by a common d-dimensional flat (or translate of a linear subspace).*

When $d = 1$ and $c = 2$, the transversal is said to be a *line-stabber* of the family of convex sets. For convenience, we refer to the target track obtained from a Markov motion process as *Markov track*.

As explained in Section II, the j^{th} Markov track consists of a set of ρ straight-line segments randomly generated according to the probability distributions of the parameters $\{\mathcal{M}_j\}_{j=1,\dots,\rho}$. When a Markov track is detected by k sensors, one or more of these segments are the stabbers of $\{\mathcal{C}_1(t), \dots, \mathcal{C}_N(t)\}$ in $\mathbb{R}^2$, possibly at different moments in time during the interval $[t_0,\ t_f]$. The temporal nature of the detections can be treated by noting that a spatio-temporal Markov track also consists of ρ three-dimensional straight-line segments in the space Ω. By definition, sensor i has a non-zero probability to detect target j at time t if and only if $||s_i(t) - p_j(t)|| \leq r_i$. Thus, the family of segments that are stabbers of the disk $\mathcal{C}_i(t)$ in $\mathbb{R}^3_+$, at t, can be represented

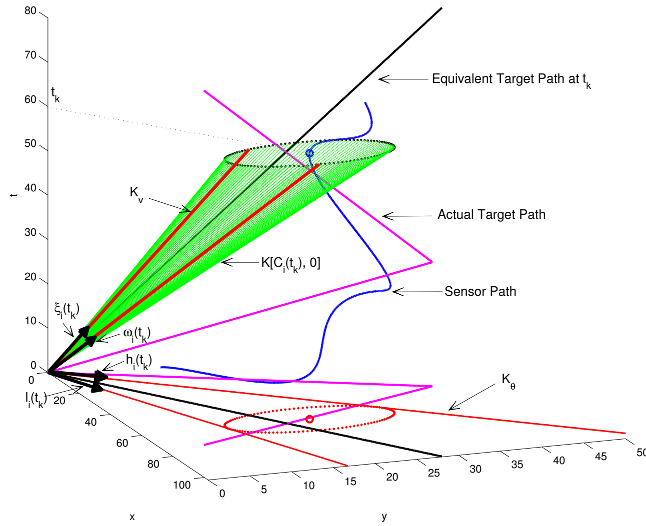

Fig. 2. Coverage cone K (green) and two-dimensional representations K_θ and K_v (red), with generating unit vectors, at time t_k [20].

by a three-dimensional generalized cone parameterized by,

$$\begin{bmatrix} x \\ y \\ t \end{bmatrix} = p_{0_j} + t_k \begin{bmatrix} r_i \cos\theta_j \\ r_i \sin\theta_j \\ 1 \end{bmatrix} \qquad (5)$$

and with a random vertex p_{0_j}. The cone in (5), denoted by $K[\mathcal{C}_i(t), p_{0_j}]$, contains all combinations of target headings and velocities that would cause a detection at t_k and, thus, it is referred to as *coverage cone*. An example of coverage cone is plotted numerically in Fig. 2 for $t_k = 60$, $s_{x_i} = 70$, and $s_{y_i} = 20$.

An efficient representation for $K[\mathcal{C}_i(t), p_{0_j}]$ consists of two 2D cones (illustrated by red lines in Fig. 2). The first, the heading plane, is obtained from the coverage cone's projection onto $\mathcal{A}$. The projection of $K[\mathcal{C}_i(t), p_{0_j}]$ onto $\mathcal{A}$ is a two-dimensional cone $K_\theta[\mathcal{C}_i(t), p_{0_j}]$ with an opening angle $\psi_i = 2\alpha_i$, where,

$$\alpha_i(t) = \sin^{-1}\left[\frac{r_i}{||s_i(t) - p_{0_j}||}\right]. \qquad (6)$$

$K_\theta[\mathcal{C}_i(t), p_{0_j}]$, abbreviated by K_θ for simplicity, is generated by the unit vectors,

$$\hat{h}_i(t) = \begin{bmatrix} \cos\alpha_i(t) & -\sin\alpha_i(t) \\ \sin\alpha_i(t) & \cos\alpha_i(t) \end{bmatrix} \frac{p_i(t)}{||p_i(t)||} \qquad (7)$$

and,

$$\hat{l}_i(t) = \begin{bmatrix} \cos\alpha_i(t) & \sin\alpha_i(t) \\ -\sin\alpha_i(t) & \cos\alpha_i(t) \end{bmatrix} \frac{p_i(t)}{||p_i(t)||}, \qquad (8)$$

where $p_i(t) \equiv s_i(t) - p_{0_j}$. K_θ is referred to as the *heading cone* because it contains all target heading angles that would cause a detection at t by sensor i.

The second, the velocity plane, defined as,

$$(\sin\theta_j)x + (\cos\theta_j)y = 0 \qquad (9)$$

contains the t-axis and is perpendicular to $\mathcal{A}$. It represents the space of all spatio-temporal target positions with a heading θ_j.

The intersection of $K[\mathcal{C}_i(t), p_{0_j}]$ with the velocity plane (9) is referred to as the *velocity cone* because it contains all target velocities along a particular heading that would cause a detection by sensor i at t. It is a two-dimensional cone denoted by $K_v[\mathcal{C}_i(t), p_{0_j}, \theta_j]$, and abbreviated by K_v, for all $\theta_j \in K_\theta$. Where, $\theta_j \in K_\theta$ is a shorthand notation for target headings that satisfy the inequality

$$[\tan^{-1}(s_{y_i}/s_{x_i}) - \alpha_i] \leq \theta_j \leq [\tan^{-1}(s_{y_i}/s_{x_i}) + \alpha_i] \quad (10)$$

Then, K_v is generated by the unit vectors,

$$\hat{\xi}_i(t) = \begin{bmatrix} \cos\theta_j \sin[\pi/2 - \eta_i(t)] \\ \sin\theta_j \sin[\pi/2 - \eta_i(t)] \\ \cos[\pi/2 - \eta_i(t)] \end{bmatrix} \quad (11)$$

and,

$$\hat{\omega}_i(t) = \begin{bmatrix} \cos\theta_j \sin[\pi/2 - \mu_i(t)] \\ \sin\theta_j \sin[\pi/2 - \mu_i(t)] \\ \cos[\pi/2 - \mu_i(t)] \end{bmatrix}, \quad (12)$$

where

$$\eta_i, \mu_i = \tan^{-1}\left[\frac{1}{v_i^{min}, v_i^{max}}\right] \quad (13)$$

$$\begin{aligned} v_i^{min}, v_i^{max} &= \frac{1}{t}\Big[s_{x_i}\cos\theta_j + s_{y_i}\sin\theta_j \quad (14) \\ &\quad \mp\sqrt{r_i^2 - (s_{x_i}\sin\theta_j + s_{y_i}\cos\theta_j)^2}\Big]. \end{aligned}$$

v_i^{min} and v_i^{max} represent the minimum and maximum target velocities that would result in a detection at t by sensor i for a particular $\theta_j \in K_\theta$. If $\theta_j \notin K_\theta$, then there will not be a detection for any target velocity. The cone K, its two-dimensional representations K_θ and K_v, and the generating unit vectors are computed and plotted in Fig. 2 for a sample time t_k, and for $p_{0_j} = 0$.

Since K_θ and K_v contain all possible straight tracks that are detected by sensor i at time t, the sum of their opening angles,

$$\begin{aligned} \psi_i(t) &= \sin^{-1}||\hat{l}_i(t) \times \hat{h}_i(t)|| \quad (15) \\ &= H(\det[\hat{l}_i(t) \quad \hat{h}_i(t)]^T)\sin^{-1}(\det[\hat{l}_i(t) \quad \hat{h}_i(t)]^T) \end{aligned}$$

and,

$$\begin{aligned} \zeta_i(t) &= \sin^{-1}||\hat{\omega}_i(t) \times \hat{\xi}_i(t)|| \quad (16) \\ &= H(\det[\hat{\omega}_i(t) \quad \hat{\xi}_i(t)]^T)\sin^{-1}(\det[\hat{\omega}_i(t) \quad \hat{\xi}_i(t)]^T) \end{aligned}$$

is a Lebesgue measure over the set of stabbers of $\mathcal{C}_i(t)$, and can be used in calculating the probability of detection of unobserved tracks. All coplanar unit vectors are ordered based on the orientation of an inertial reference frame such that two coplanar vectors $u_i \prec u_j$ if when these vectors are translated such that their origins coincide, and u_i is rotated through the smallest possible angle to meet u_j, this orientation is in the same direction as the orientation of the reference frame. Thus, the Heaviside function $H(\cdot)$ in (15) and (16) ensures that if $\hat{l}_i(t) \succ \hat{h}_i(t)$, or $\hat{\omega}_i(t) \succ \hat{\xi}_i(t)$, the corresponding opening angles are equal to zero.

It can be seen from (3),(6)-(16), that the opening angles of the heading and velocity cones can be written as explicit functions of the sensor position, and of the target position at the discontinuities, i.e., $\psi_i = \psi_i[s_i(t), p_{0_j}]$ and $\zeta_i = \zeta_i[s_i(t), p_{0_j}, \theta_j]$. For unobserved tracks, the Markov motion parameters $\mathcal{M}_j$ can be assumed independent and uniformly distributed. Thus, the joint probability mass function (PMF) between two consecutive discontinuities (or maneuvering time instants) $f_t(t_j, t_{j+1})$ is uniformly distributed over discrete time intervals Δt_j, $j = 1, \ldots, \rho$, with values defined by the user. During every time interval, the target heading has a probability density function (PDF) $f_\theta(\theta_j)$ that is uniform over the interval $\mathcal{I}_{\theta_{j-1}} \equiv [\theta_{j-1} - \pi/2, \ \theta_{j-1} + \pi/2]$, due to a maximum turning radius of $\pi/2$. The velocity of every target has a PDF $f_v(v_j)$ that is uniform over the interval $[v_i^{min}, \ v_i^{max}]$, with $v_i^{min} > 0$. The probability that sensor i obtains a detection at time, t_k is then,

$$\begin{aligned} P_d^i(t_k) &= \int_{p_{0_j} \in \mathcal{A}} f_{xy}(p_{0_j}) \quad (17) \\ &\quad \times \int_{\gamma_i}^{\lambda_i} \int_{1/\tan(\eta_i)}^{1/\tan(\mu_i)} f_{\theta v}(\theta_{eq}, v_{eq}) dv_{eq} d\theta_{eq} dp_{0j}, \end{aligned}$$

where $f_{\theta v}(\theta_{eq}, v_{eq})$ is the derived joint probability density distribution of the equivalent course and speed (4). Using the theory of derived distributions [21] and the transformation in (4), $f_{\theta v}(\theta_{eq}, v_{eq})$ can be computed from the original transition probability density functions $\{\Pr(\theta_j, v_j, t_j)\}_{j=1,\ldots,\rho}$ provided in rectangular coordinates. A benefit of this type of numerical integration is that the probability density functions for the target's Markov parameters do not need to be static or independent.

Since each sensor has a detection radius, $r_i > 0$, individual detections will normally come in batches as the target passes through a sensor's detection disk. Therefore, detection events at different moments in time do not constitute disjoint events because they are not mutually exclusive, and are highly correlated. As a result, adding the values of $P_d(t)$ over time does not result in a probability function. Let D_i be a binary variable whose value can be only 0 or 1, and are mutually exclusive. $D_i(t) = 1$ occurs when a detection is made by the i^{th} sensor at time t, and $D_i(t) = 0$ occurs when no detection occurs by the i^{th} sensor at time t. Thus, $P_d^i(t)$ is the probability of $D_i(t) = 1$ at time t, and the probability that $D_i(t) = 0$ is $[1 - P_d^i(t)]$. It then follows that the expected value of D_i at time t is,

$$E[D_i(t)] = 1 \cdot P_d^i(t) + 0 \cdot [1 - P_d^i(t)] = P_d^i(t) \quad (18)$$

where $E[\cdot]$ denotes expectation. To find the expected number of detections over the time interval $[t_0, \ t_f]$, equation (17) can be integrated over time. In the presence of $i = 1, 2, \ldots, n$ sensors, each with a known deterministic trajectory, the total number of detections is given by,

$$J_i \triangleq \sum_{t_k = t_0}^{t_f} D_i(t_k) dt \quad (19)$$

where t_k denotes a time instant in the discretized time interval $[t_0,\ t_f]$. Combined with (17), the above equation provides the total number of detections expected for sensor i.

$$E[J_i] = \sum_{i=1}^{n} \sum_{t_0}^{t_f} \int_{p_{0_j} \in \mathcal{A}} f_{xy}(p_{0_j}) \times \int_{\gamma_i}^{\lambda_i} \int_{1/\tan(\eta_i)}^{1/\tan(\mu_i)} f_{\theta v}(\theta_{eq}, v_{eq}) dv_{eq} d\theta_{eq} dp_{0_j} dt \quad (20)$$

The expected total number of detections for the sensor network (20) is then obtained by summing (19) over $i = 1, \ldots, n$. In the next section, this approach is validated graphically using a Monte Carlo simulation involving multiple mobile sensors and multiple mobile targets.

IV. Simulations and Results

Monte Carlo (MC) simulations are a flexible and effective approach for evaluating the effects of uncertainty propagation on the system performance for one or more uncertain parameters with known probability density functions (PDFs) [22], [23]. For the stochastic problem formulated in Section II, a Markov target is generated by sampling the joint probability density function to obtain instantiations of the Markov parameters over the period $[t_0, t_f]$. The maneuvering target's equivalent course and speed can then be calculated using (4). From these sample parameters, a sample trajectory for the maneuvering target can be computed using (3). Once the target trajectory is known, the sensor detections can be determined by direct evaluation of the detection events D_j at every intersection between the target trajectory and the sensor FOV. By repeating this procedure and evaluating the target trajectory an adequate number of times, M, to generate a statistically significant sample size for the joint probability density function of the Markov parameters, a Monte Carlo simulation of the maneuvering targets in the region of interest can be obtained.

A logical array or truth table, denoted by B_j, is evaluated such that every element corresponds to one instantiation of the Markov parameters $\mathcal{M}$, and is set equal to 1 or 0, depending on whether the track has been detected (1) or missed (0) by the j^{th} sensor. After the array B_j is obtained for every sampled sensor, the logical array,

$$T_k = \left\{ \sum_{j=1}^{n} B_j \geq k \right\} \quad (21)$$

indicates whether each possible track in $\mathcal{A}$ has been detected by at least k sensors. Then, the number of ones in T_k divided by its number of elements provides the estimate P_k for the probability of track detection. Figure 3 illustrates a few samples of Markov target trajectories and the positions of four stationary sensors, with corresponding detections over the entire time frame. However, once moving sensors are incorporated, a 2-dimensional representation no longer adequately reflects the spatio-temporal dependance of detection opportunities. Figure 4 illustrates this by showing the

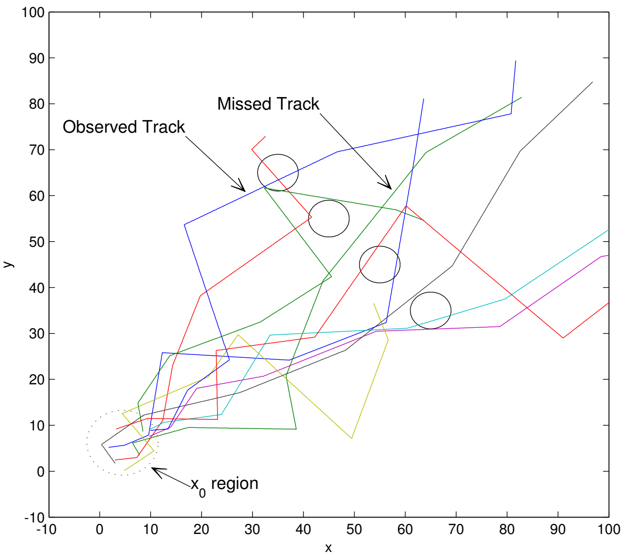

Fig. 3. Ten possible Markov target tracks and four stationary sensors.

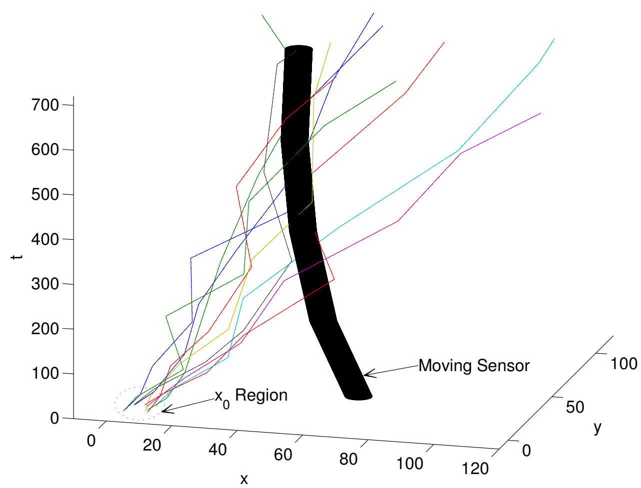

Fig. 4. Ten possible Markov target tracks and one moving sensor.

detections of one moving sensor over time for a small sample of Markov target trajectories, as the trajectories intersect the sensors' FOVs in a three-dimensional spatio-temporal Euclidian space. By this approach, the MC simulation can be used to validate the closed-form track coverage function (20) derived in Section III, for known sensors' trajectories and speeds (1). As shown, in Figs. 5-6, the extended geometric transversals approach developed in this paper leads to the same probability of detection as the Monte Carlo simulation across the entire span of time, or at specific instants. The same figures, in fact, are obtained by means of the track coverage function (20), indicating that the track coverage approach presented in this paper can be utilized to determine sensor detections of maneuvering targets for any Markov parameters and sensor trajectories in spatio-temporal space.
Figure 7 illustrates four snapshots of the time progression of a maneuvering target in the ROI – with Markov parameters

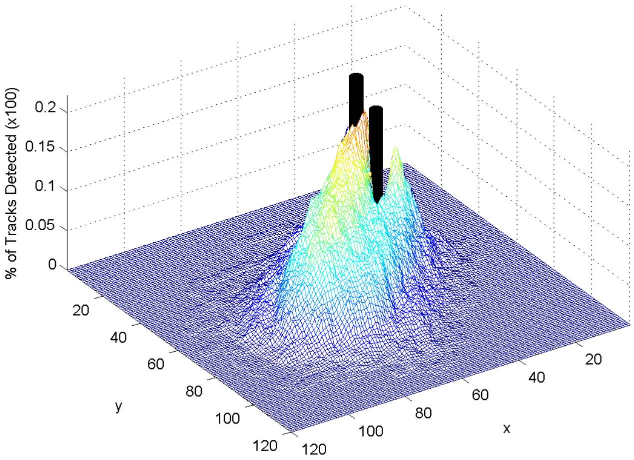

Fig. 5. Probability of track detection from t=0 through t=t_f for a maneuvering target with known joint probability density function , against two stationary sensors.

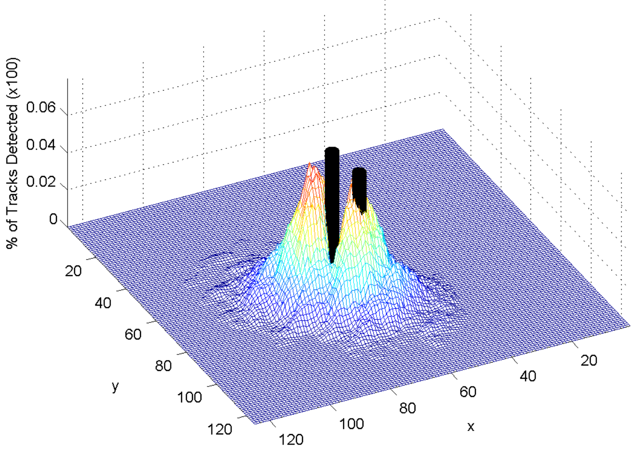

Fig. 6. Probability of track detection at $t = 9$s for a maneuvering target with known joint probability density function, and two sensors' known instantaneous positions.

sampled from the same joint probability function used in Figs. 5-6, and shown in Fig. 3 – and four moving sensors with detections precisely predicted by the track coverage approach at several instants in time, such as $t = 7$ s and $t = 7.9$ s. Hence, the extended approach presented in this paper can be utilized to optimize and control sensor networks deployed to detect maneuvering targets, based on the joint probability density functions obtained from established tracking and estimation algorithms.

V. Conclusion

This paper presents an extended approach based on convex theory and computational geometry to obtain a track coverage function for maneuvering targets in the plane. This method uses line transversals and planar geometry to derive the track coverage of a heterogeneous sensor network as a function of the Markov transition probability functions. The planar geometric transversals approach is extended to a three-dimensional Euclidian space representing the sensor-target spatio-temporal coordinates, in which the Markov parameters of detected maneuvering targets can be represented by three-dimensional cones finitely generated by the sensors' fields-of-view. When the target tracks are represented by piece-wise Markov motion models the sensor network can estimate the target state from multiple, distributed sensor measurements. This closed-form representation of the probability of track detection is a function of these transition probabilities, and it accounts for the spatio-temporal trajectories of both the sensors and the targets, any sensor dynamics, and any form of the target probability density functions. The approach is demonstrated through simulations involving both stationary and maneuvering sensors attempting to detect the same set of maneuvering targets.

References

[1] V. Isler, S. Khanna, and K. Daniilidis, "Sampling based sensor-network deployment," *Proc. IEEE/RSJ Int. Conf. on Intelligent Robots and Systems*, vol. 100, pp. 1780–1785, 2004.

[2] J. Cortés, S. Martínez, T. Karatas, and F. Bullo, "Coverage control for mobile sensing networks," *IEEE Transactions on Robotics and Automation*, vol. 20, no. 2, pp. 243–255, April 2004.

[3] J. O'Rourke, *Art Gallery Theorems and Algorithms*. New York, NY: Oxford University Press, 1987.

[4] A. Ganguli, J. Cortés, and F. Bullo, "Maximizing visibility in nonconvex polygons: Nonsmooth analysis and gradient algorithm design," *SIAM Journal on Control and Optimization*, vol. 45, no. 5, pp. 1657–1679, 2006.

[5] J. Urritia, "Art gallery and illumination problems," in *Handbook on Computational Geometry*, J. Sack and J. Urritia, Eds. Boca Raton, FL: Elsevier Science Publishers, 1992, pp. 387–434.

[6] J.-P. LeCadre and G. Souris, "Searching tracks," *IEEE Transactions on Aerospace and Electronic Systems*, vol. 36, no. 4, pp. 1149–1166, 2000.

[7] T. A. Wettergren, "Performance of search via track-before-detect for distributed sensor networks," *IEEE Trans. on Aerospace and Electronic Systems*, vol. 44, no. 1, pp. 314–325, 2008.

[8] K. C. Baumgartner and S. Ferrari, "A geometric transversal approach to analyzing track coverage in sensor networks," *IEEE Trans. on Computers*, vol. 57, no. 8, pp. 1113–1128, 2008.

[9] K. C. Baumgartner, S. Ferrari, and T. Wettergren, "Robust deployment of dynamic sensor networks for cooperative track detection," *IEEE Sensors*, vol. 9, no. 9, pp. 1029–1048, 2009.

[10] K. C. Baumgartner, S. Ferrari, and A. Rao, "Optimal control of an underwater sensor network for cooperative target tracking," *IEEE Journal of Oceanic Engineering*, vol. 34, no. 4, pp. 678–697, 2009.

[11] M. Xiang and J. Zhao, "On the performance of distributed neyman-pearson detection systems," *IEEE Transactions in Systems, Man and Cybernetics - Part A*, vol. 31, no. 1, pp. 78–83, January 2001.

[12] M. Ranasingha, M. Murthi, K. Premaratne, and X. Fan, "Transmission rate allocation in multisensor target tracking over a shared network," *IEEE Transactions on Systems, Man and Cybernetics - Part B*, vol. 39, no. 2, pp. 348–362, 2009.

[13] S. Ferrari, R. Fierro, B. Perteet, C. Cai, and K. Baumgartner, "A geometric optimization approach to detecting and intercepting dynamic targets using a mobile sensor network," *SIAM Journal on Control and Optimization*, vol. 48, no. 1, pp. 292–320, 2009.

[14] B. Perteet, J. McClintock, and R. Fierro, "A multi-vehicle framework for the development of robotic games: The Marco Polo case," in *Proceedings of the IEEE International Conference on Robotics and Automation*, Rome, Italy, April 10-14 2007, pp. 3717–3722.

[15] S. Ferrari, C. Cai, R. Fierro, and B. Perteet, "A multi-objective optimization approach to detecting and tracking dynamic targets in pursuit-evasion games," New York, NY, 2007, pp. 5316–5321.

[16] T. A. Wettergren and R. Costa, "Optimal placement of distributed sensors against moving targets," *ACM Transactions on Sensor Networks*, vol. 5, no. 3, p. Article 26, May 2009.

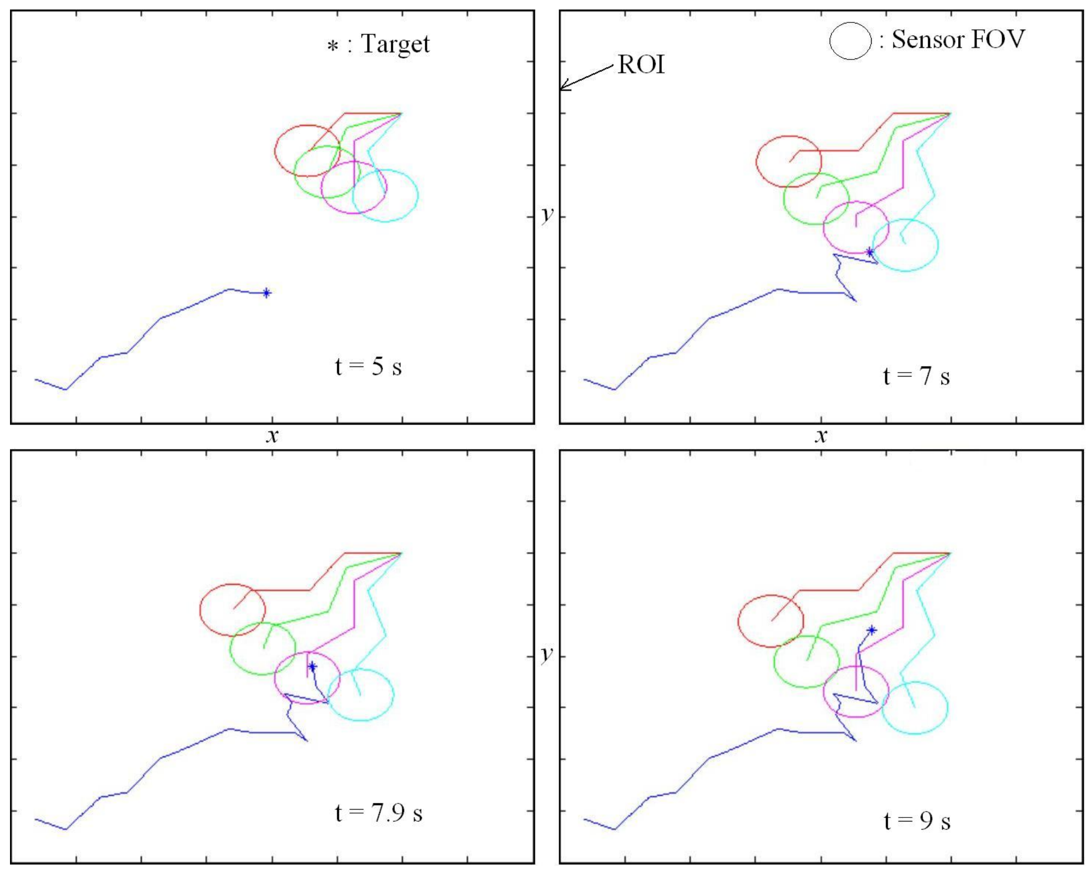

Fig. 7. Snapshots of time progression of a maneuvering target in the ROI, with a sampled Markov trajectory shown in Fig. 3, and four moving sensors with detections precisely predicted by the track coverage approach at several instants in time, such as $t = 7$ s and $t = 7.9$ s.

[17] Y. Bar-Shalom, X. R. Li, and T. Kirubarajan, *Estimation with applications to tracking and navigation: Algorithms and software for information extraction*. John Wiley and Sons, 2001.

[18] J. Gubner, *Probability and Random Processes for Electrical and Computer Engineers*. Cambridge, UK: Cambridge University Press, 2006.

[19] J. E. Goodman, R. Pollack, and R. Wenger, "Geometric transversal theory," in *New Trends in Discrete and Computational Geometry*, J. Pach, Ed. Springer Verlag, 1991, pp. 163–198.

[20] S. Ferrari, R. Fierro, and D. Tolic, "A geometric optimization approach to tracking maneuvering targets using a heterogeneous mobile sensor network," *Proceedings of the 48th IEEE Conference on Decision and Control*, pp. 1080–1087, 2009.

[21] J. Pitman, *Probability*. New York, NY: Springer-Verlag, 1993.

[22] R. F. Stengel and L. R. Ray, "Stochastic robustness of linear time-invariabt control systems," *IEEE Transactions on Automatic Control*, vol. 36, no. 1, pp. 82–87, 1991.

[23] R. Y. Rubinstein, *Simulation and the Monte Carlo Method*. New York, NY: John Wiley and Sons, 1981.